

## Supplementary Information

### Cu<sup>I</sup>-Cu<sup>II</sup> and Ag<sup>I</sup> *p*-isocyanobenzoates as novel 1D semiconducting coordination oligomers

Leslie Reguera<sup>a,d,f,\*</sup>, Arely Cano<sup>a,b</sup>, Joelis Rodríguez-Hernández<sup>c</sup>, Daniel G. Rivera<sup>f</sup>, Erik V. Van der Eycken<sup>d,e</sup>, Daniel Ramírez-Rosales<sup>g</sup> and Edilso Reguera<sup>a\*</sup>

- a* Instituto Politécnico Nacional, Centro de Investigación en Ciencia Aplicada y Tecnología Avanzada, U. Legaria, Ciudad México, México; E-mail: edilso.reguera@gmail.com
- b* Fermi National Accelerator Laboratory, Batavia, IL, 60510, United States
- c* Centro de Investigación en Química Aplicada, Saltillo, Coahuila, México.
- d* Laboratory for Organic & Microwave-Assisted Chemistry (LOMAC), Department of Chemistry, University of Leuven (KU Leuven), Belgium.
- e* Peoples' Friendship University of Russia (RUDN University), 6 Miklukho-Maklaya street, Moscow, 117198 (Russia)
- f* Universidad de La Habana, Facultad de Química, La Habana, Cuba; E-mail: [lesliereguera2005@gmail.com](mailto:lesliereguera2005@gmail.com)
- g* Instituto Politécnico Nacional, ESFM, Ave. Instituto Politécnico Nacional S/N, Edif. 9 U.P. Zacatenco, Col. San Pedro Zacatenco, Mexico City, 07738, Mexico

### Table of Content

1. <sup>1</sup> H-NMR and <sup>13</sup> C-NMR of K-ICNBA ligand	2
2. Details on the XRD data recording and processing, refined atomic positions, thermal ( <i>B</i> <sub>iso</sub> ) and occupation ( <i>Occ</i> ) factors, and calculated inter-atomic distances and bond angles from the refined structure	3
3. Spectroscopic characterization of Cu <sup>I</sup> Cu <sup>II</sup> -ICNBA and Ag <sup>I</sup> -ICNBA by IR, Raman XPS, and UV-vis-NIR.	5
4. Thermogravimetric analysis of K-ICNBA, Cu <sup>I</sup> Cu <sup>II</sup> -ICNBA, and Ag <sup>I</sup> -ICNBA	9
5. Optoelectronic characterization of Cu <sup>I</sup> Cu <sup>II</sup> -ICNBA and Ag <sup>I</sup> -ICNBA by UV-vis-NIR data processing	10

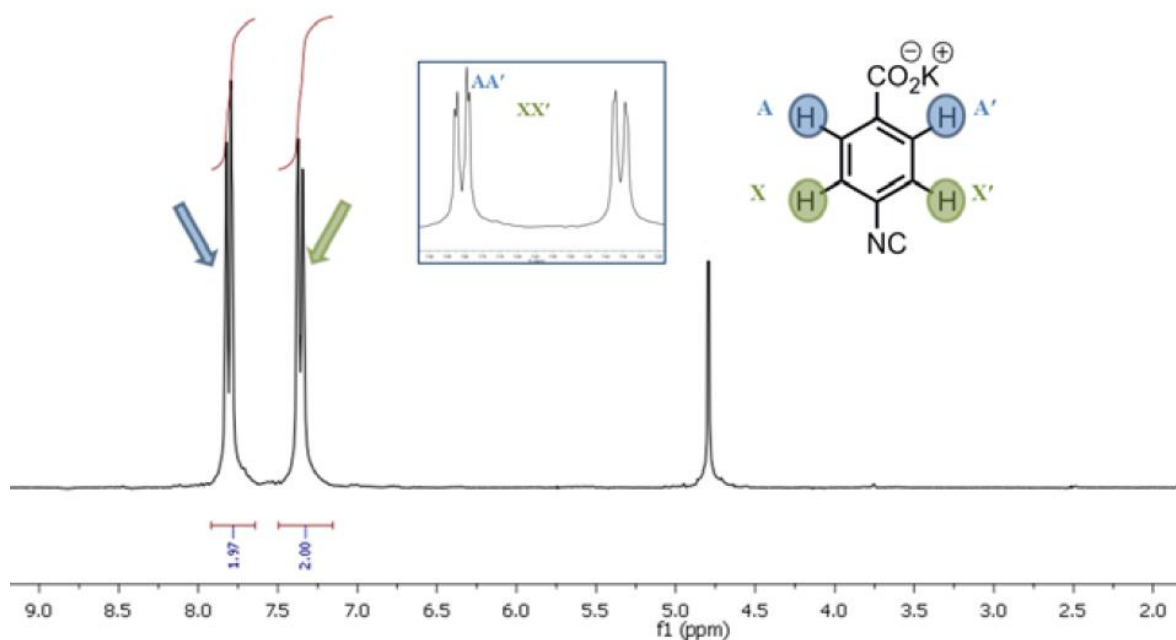


Figure S1.  $^1\text{H-NMR}$  of K-ICNBA

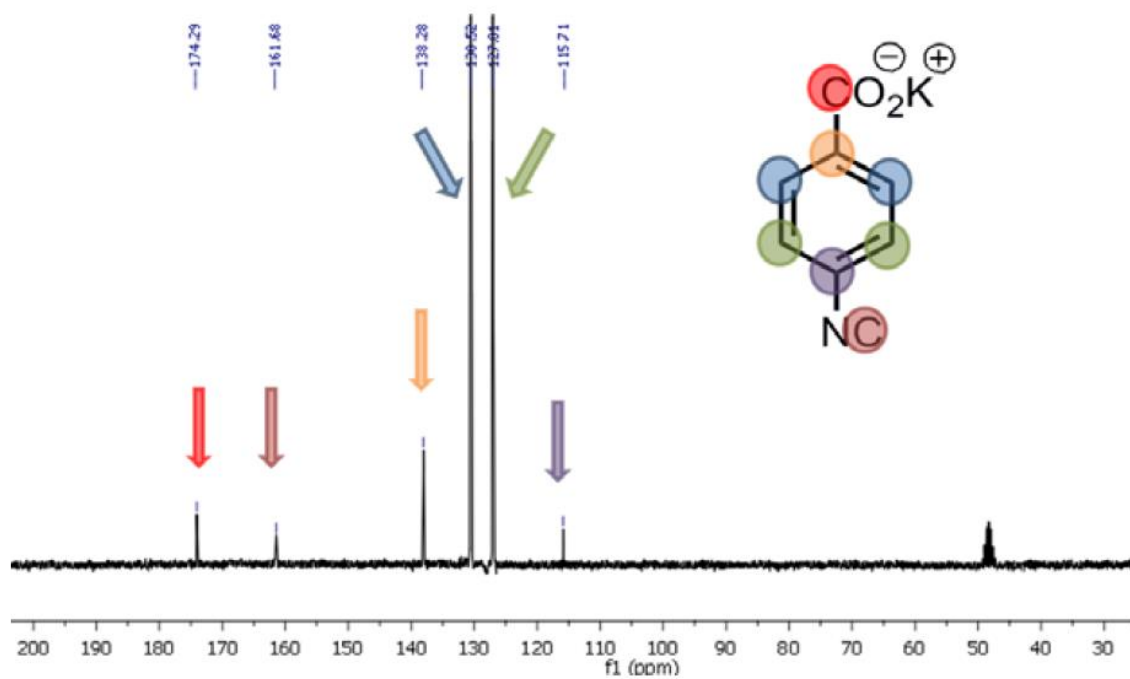


Figure S2.  $^{13}\text{C-NMR}$  of K-ICNBA

## 2. Details on the XRD data recording and processing

The X-ray powder pattern of Ag<sup>I</sup>-ICNBA was indexed using the programs N-TREOR90<sup>1</sup> and DICVOL<sup>2</sup> indicating a monoclinic unit cell:  $a = 11.504(1) \text{ \AA}$ ,  $b = 10.129(1) \text{ \AA}$ ,  $c = 7.604(1) \text{ \AA}$ ,  $\beta = 123.29(1)^\circ$ . The figures of merit were  $M(20) = 27$  and  $F(20) = 36$ . These cell parameters were refined by the Le Bail method<sup>3</sup> implemented in the FULLPROF<sup>4</sup> program. Space group assignment was made based on the systematic absences and the fact that  $Z = 4$ . However, it was not possible to unambiguously determine the space group, and all possibilities were then tested. The structure to be refined was determined by direct methods using the program EXPO2009.<sup>5</sup> By the application of the direct methods, the best results were obtained for the  $C2/c$  space group, obtaining from this model the starting atomic position used for the refinement. This model was refined by the Rietveld method implemented in the FULLPROF<sup>4</sup> program. In the final refinement, all atomic positions were allowed to vary and the occupation factor of the atoms in the carboxylate and isocyanide groups were refined dependently. The thermal parameters were refined in the same way, that is, dependently for the light atoms and independently for Ag.

**Table S1.** Experimental details for the XRD data recording and processing for Ag<sup>I</sup>-ICNBA

<b>Ag<sup>I</sup>-ICNBA</b>	
<b>Data collection</b>	
Diffractometer	Bruker, D8 Advance
Detector	Linx Eye
Wavelength (Å)	CuKα <sub>1</sub> , 1.54056
2θ range (°)	10-70
Step size (°)	0.02
Time per step (s)	26
<b>Unit cell</b>	
Space Group	C2/c
Parameter (Å)	a= 11.504(1)
	b= 10.129(1)
	c= 7.604(1)
	β=123.29(1)°
V(Å <sup>3</sup> )	740.61(14)
Z	4
<b>Refinement</b>	
# of reflections	165
# of distance constraints	1
<b># of refined parameters</b>	
Structural	29
Profile	12
Rexp	5.31
Rwp	11.2
RB	9.84
S	2.10

**Table S2.** Refined atomic positions and thermal ( $B_{iso}$ ) and occupation (Occ) factors for Ag<sup>I</sup>-ICNBA

Composition	site	x	y	z	Biso	Occ
Ag	4e	0.5	0.110(2)	0.25	2.61(2)	1
O1	8f	0.365(2)	0.054(4)	0.281(3)	1.80(3)	0.437(2)
O2	8f	0.263(2)	0.212(3)	0.220(3)	1.80(3)	0.437(2)
C3	8f	0.063(1)	-0.026(3)	0.242(2)	1.80(3)	1
C4	8f	0.159(3)	0.081(2)	0.274(2)	1.80(3)	1
C5	8f	0.281(2)	0.102(3)	0.288(2)	1.80(3)	0.437(2)
C6	8f	0.069(2)	0.176(3)	0.268(2)	1.80(3)	1
C2	8f	0.661(2)	0.136(2)	0.220(2)	1.80(3)	0.563(2)
N2	8f	0.753(3)	0.125(3)	0.192(2)	1.80(3)	0.563(2)

**Table S3.** Calculated interatomic distances (in Å) and bond angles (in °) from the refined structure for Ag<sup>I</sup>-ICNBA

Bond distance (Å)		Angles (°)
Ag-C2= 2.003(2)	O1-Ag-C2=169.0(2)	C6-C6'-C4'= 136.0(3)
C2-N2= 1.194(1)	Ag-C2-N2=166.7(3)	C6'-C4'-C3'= 91.5(2)
Ag-O1= 1.783(1)	Ag-O1-C5=135.3(4)	C4'-C3'-C3= 130.5(4)
Ag-O2= 2.805(1)	O1-C5-O2=109.6(2)	C3'-C3-C4= 130.5(4)
O1-C5= 1.109(1)	O1-C5-C4=144.5(4)	C2-N2-C4'=149.9(5)
C5-O2=1.198(1)	O2-C5-C4= 100.6(2)	C3-C4-C6= 91.5(2)
C5-C4=1.365(1)	C5-C4-C6= 127.4(3)	C3-C4-C5= 140.8(3)
C4-C3=1.469(1)	C4-C6-C6'= 136.0(3)	
C3-C3'=1.520(1)		
C3'-C4'= 1.469(1)		
C4'-C6'= 1.396(1)		
C6'-C6=1.455(1)		
C6-C4=1.396(1)		

<sup>^</sup>-x, y, 0.5-z

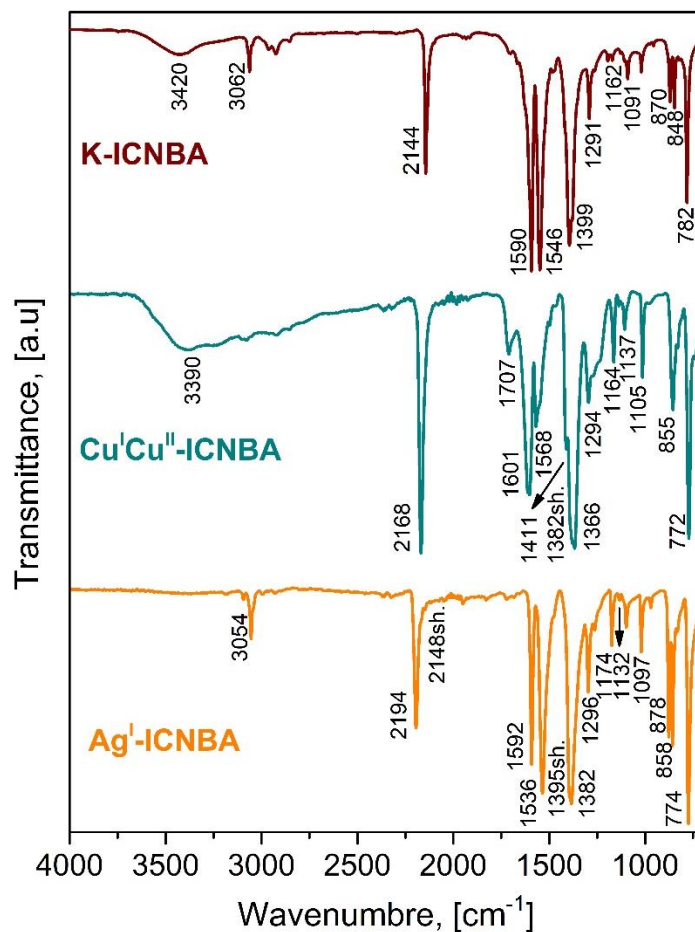


**Figure S3.** IR spectra for K-ICNBA, Cu<sup>I</sup>Cu<sup>II</sup>-ICNBA, and Ag<sup>I</sup>-ICNBA

**Table S4.** IR and Raman absorption assignment for K-ICNBA, Cu<sup>I</sup>Cu<sup>II</sup>-ICNBA, and Ag<sup>I</sup>-ICNBA. IR spectra were measured in the 4000-400 cm<sup>-1</sup> wavenumber range. Raman spectra were measured using an excitation wavelength of 455 nm, in 3500-100 cm<sup>-1</sup> Raman shift range.

Assignment	K-ICNBA		Cu <sup>I</sup> Cu <sup>II</sup> -ICNBA		Ag <sup>I</sup> -ICNBA	
	IR	IR	Raman	IR	Raman	
$\nu_{OH (H_2O)}$	3420	3390	-	-	-	
$\nu_{CH}$	3062	-	-	3054	-	
$\nu_{NC (coord.)}$	-	2168	2194, 2171	2194	2194	
$\nu_{NC (free)}$	2144	-	-	2148sh.	-	
$\delta_{benzene\ ring}$	-	-	2988	-	2988	
$\nu_{COOH}^{as}$	-	1707	-	-	-	
$\nu_{COO^-}^{as}$	1590, 1546	1601, 1568	1601	1592, 1536	1597	
$\nu_{COO^-}^s$	1399	1411, 1382sh., 1366	1411	1395sh., 1382	1395	
$\nu_{NCring}^s$	1291	1294, 1272sh., 1239sh.	-	1296, 1264	-	
$\nu_{NCring}^{as}$	1172	1164	1186, 1166	1174	1174	
$\delta_{CCC\ in\ plane}$	1162	1137	1137	1132	1132	
$\delta_{CH\ in\ plane}$	1091	1105	-	1097	-	
$\delta_{CH\ out\ of\ plane}$	848	855	-	877, 858	-	
$\delta_{CCC\ out\ of\ plane}$	782	772	-	774	-	
$\delta_{MCN}$	OMR	OMR	405	OMR	410	
$\nu_{M-CN}$	OMR	OMR	303	OMR	-	
$\delta_{CMC\ and\ \delta_{OMC}}$	OMR	OMR	189	OMR	-	

sh.: shoulder, OMR: Out of measurement range

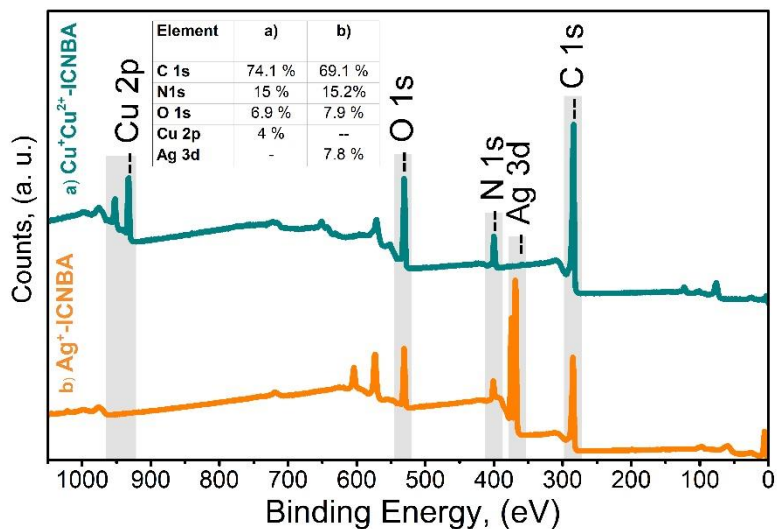


**Figure S4.** Elemental identification from XPS survey spectra for Cu<sup>I</sup>Cu<sup>II</sup>-ICNBA (top) and Ag<sup>I</sup>-ICNBA (bottom). The spectra were recorded with monochromatic Al K $\alpha$  source and 160 eV as pass energy. Both Inset: Elemental quantification in atomic percentage (At. %).

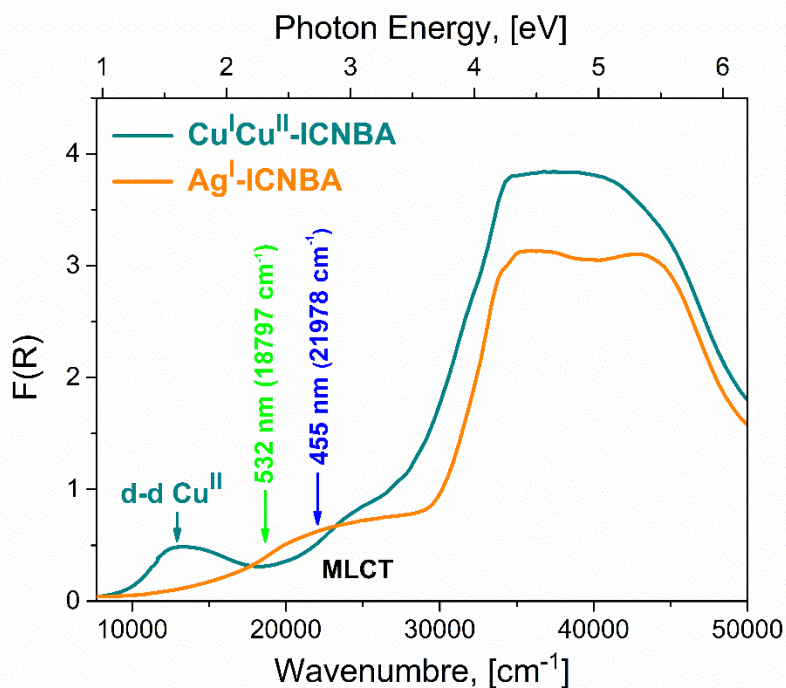


**Figure S5.** Diffuse-reflectance UV-vis-NIR spectra for Cu<sup>I</sup>Cu<sup>II</sup>-ICNBA and Ag<sup>I</sup>-ICNBA. Labeled in green and blue the excitation wavelengths using for the Raman measurements.

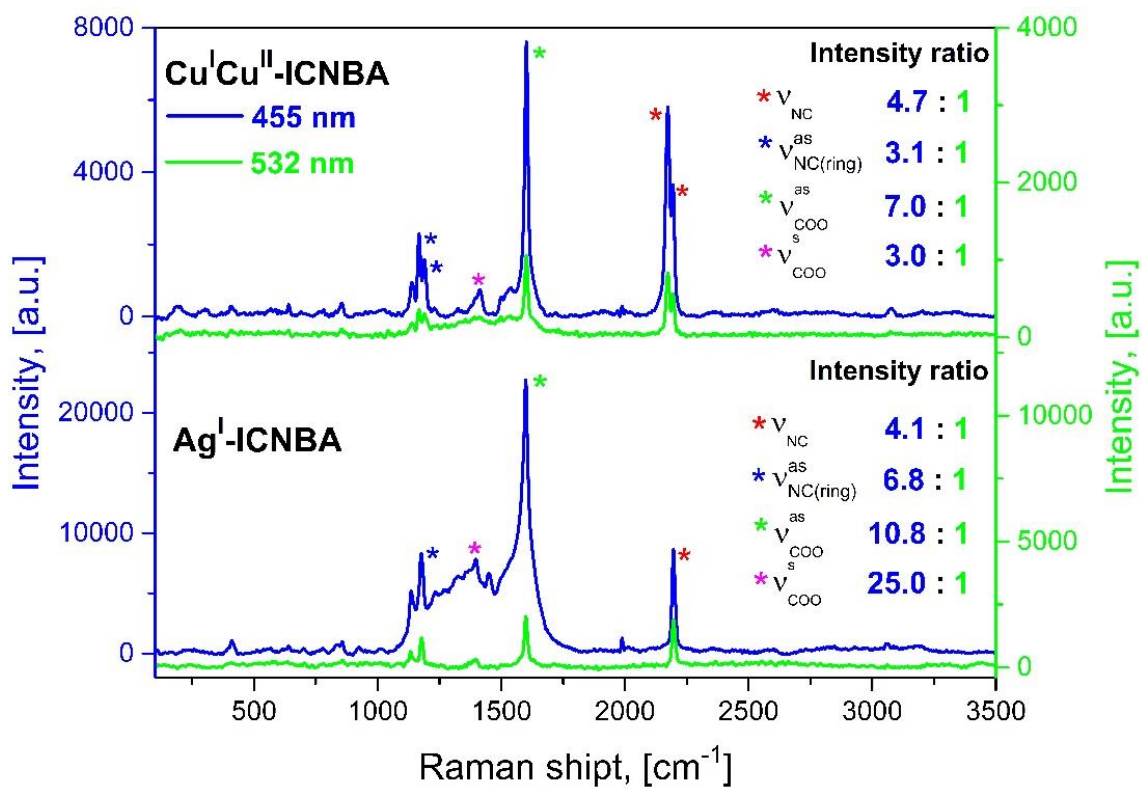


**Figure S6.** Raman spectra for Cu<sup>I</sup>Cu<sup>II</sup>-ICNBA and Ag<sup>I</sup>-ICNBA measured in- and out of resonance, using excitation wavelengths of 455 and 532 nm, respectively, Inset: the intensity ratio for each band.



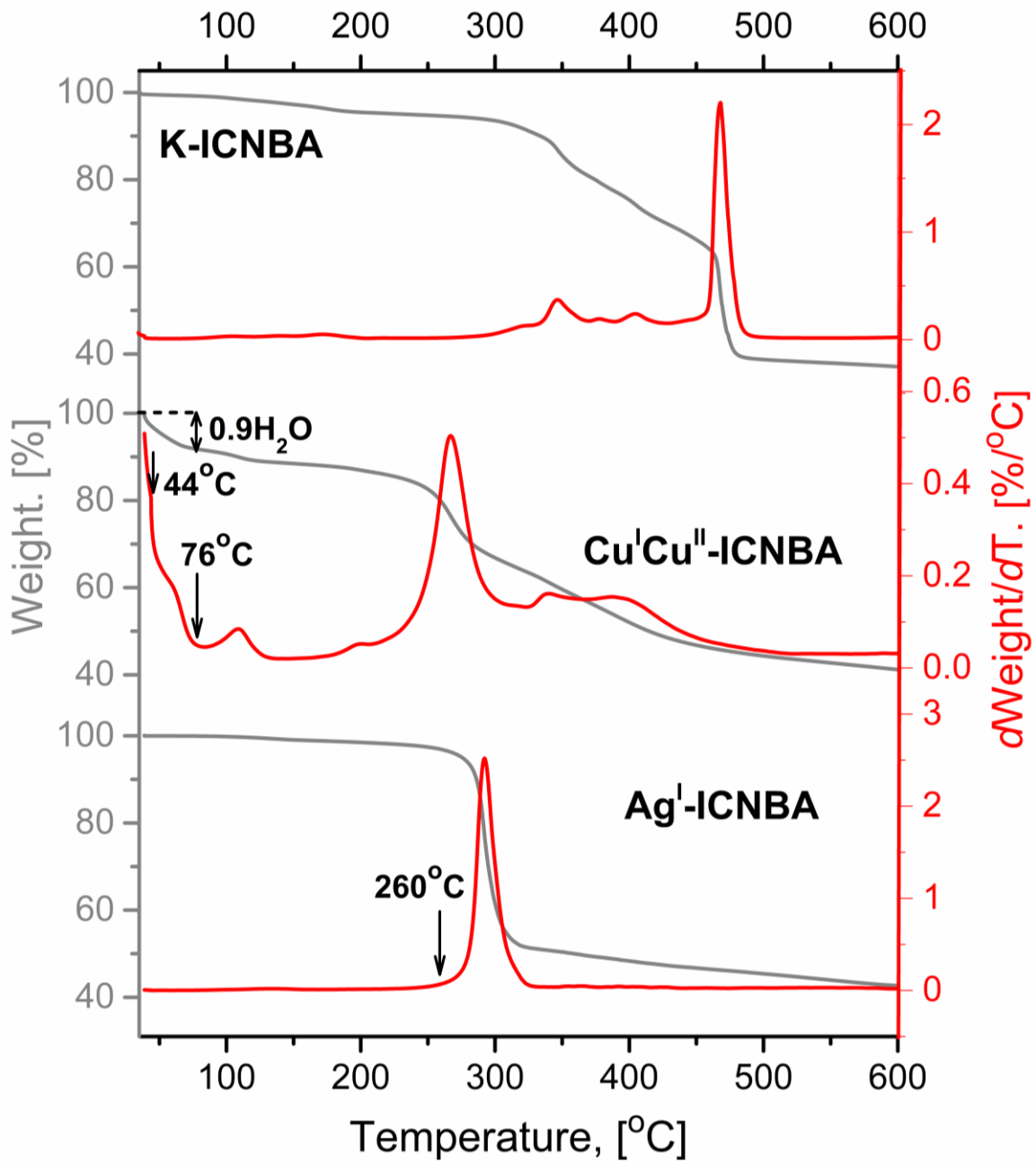


**Figure S7.** TG and DTG curves for K-ICNBA, Cu<sup>I</sup>Cu<sup>II</sup>-ICNBA, and Ag<sup>I</sup>-ICNBA.

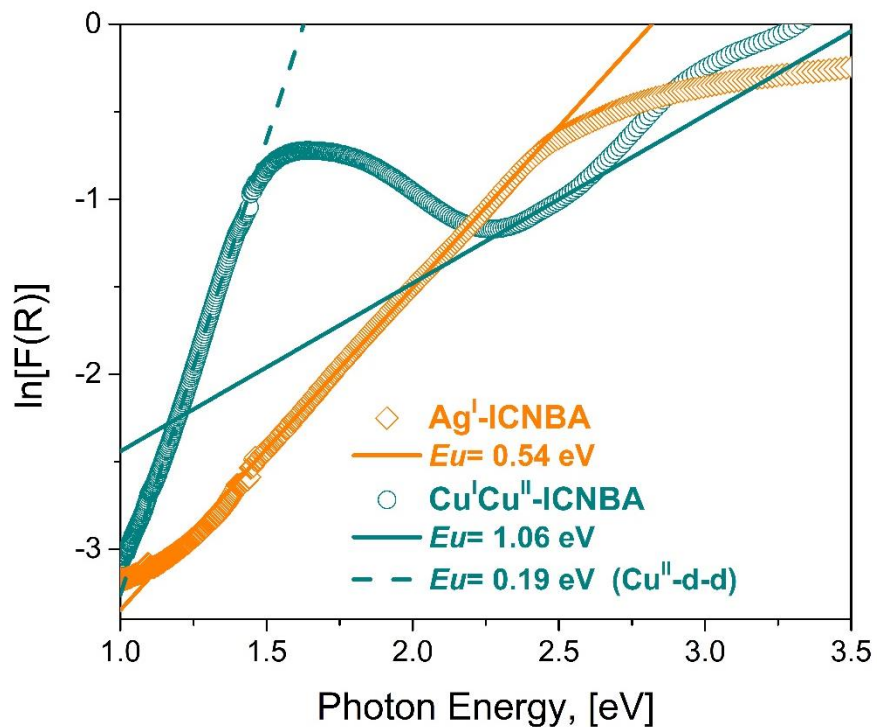


Figure S8. Urbach plot for Cu<sup>I</sup>Cu<sup>II</sup>-ICNBA and Ag<sup>I</sup>-ICNBA

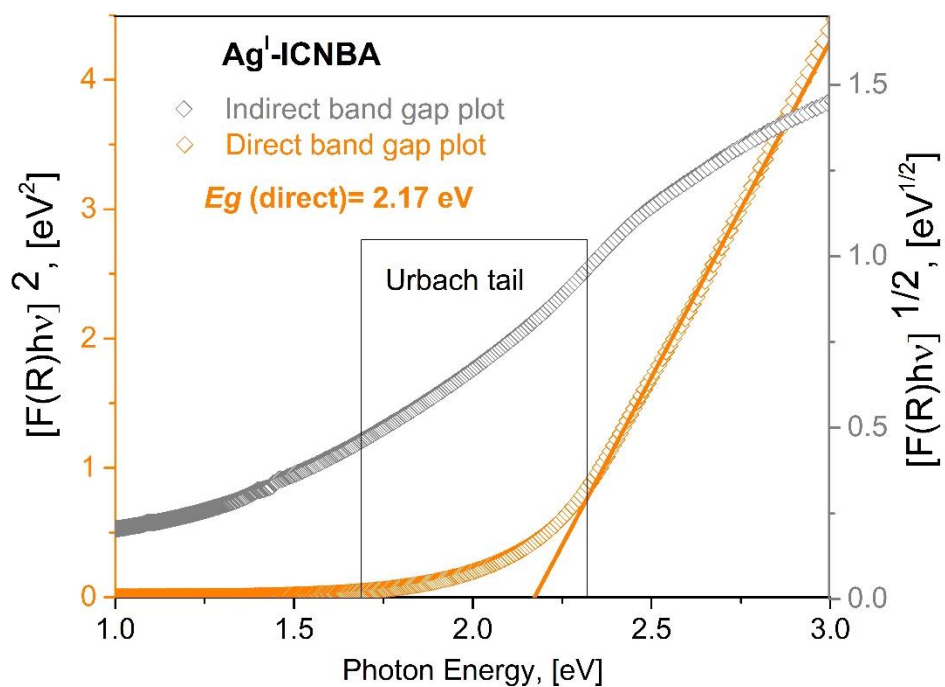
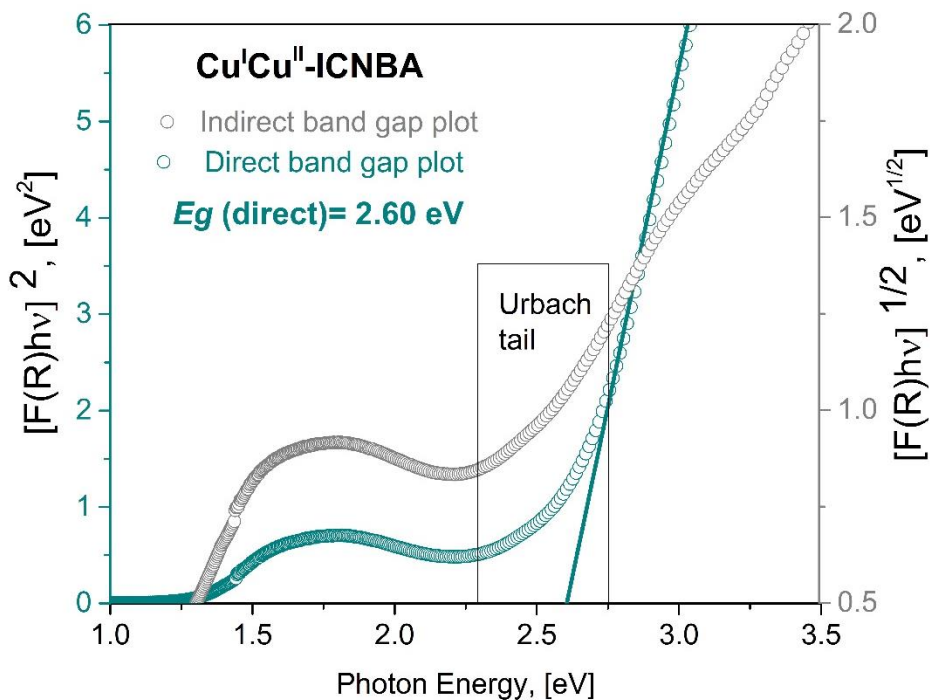
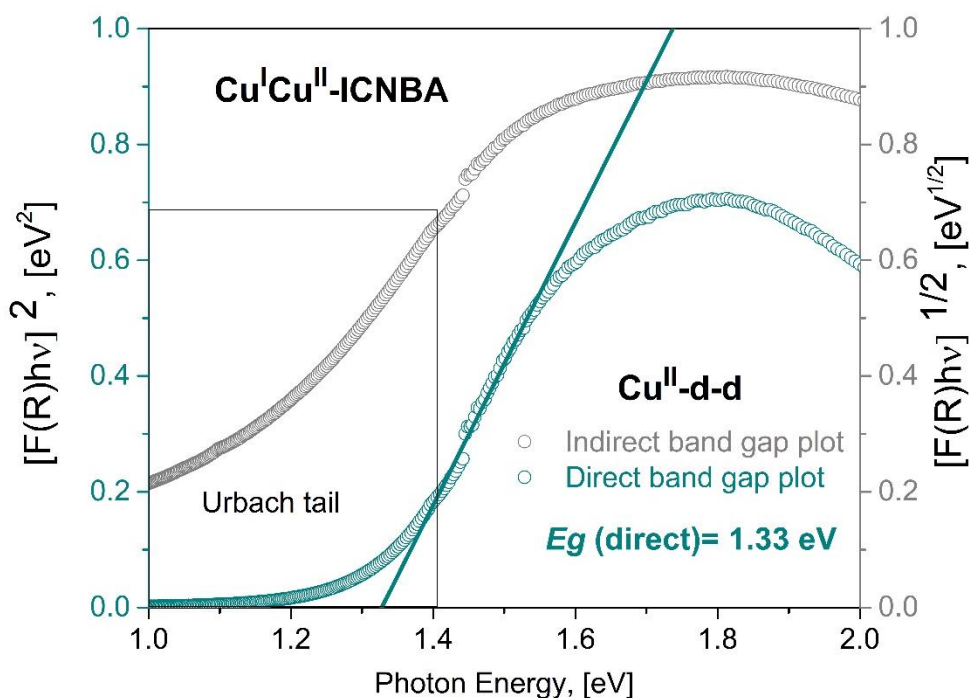


Figure S9.  $[F(R)h\nu]^{1/\eta}$  vs.  $h\nu$  plot for Ag<sup>I</sup>-ICNBA, a lineal behavior for  $\eta=1/2$  was obtained, indicating that the material behaves as a direct bandgap semiconductor. The band to band energy gap ( $E_g$ ) was calculated excluding the Urbach zone of the curve.



**Figure S10.**  $[F(R)h\nu]^{1/\eta}$  vs.  $h\nu$  plot for  $\text{Cu}^{\text{I}}\text{Cu}^{\text{II}}\text{-ICNBA}$ , a lineal behavior for  $\eta=1/2$  was obtained, indicating that the material behaves as a direct bandgap semiconductor. The band to band energy gap ( $E_g$ ) was calculated excluding the Urbach zone of the curve.



**Figure S11.**  $[F(R)h\nu]^{1/\eta}$  vs.  $h\nu$  plot for  $\text{Cu}^{\text{I}}\text{Cu}^{\text{II}}\text{-ICNBA}$ , a lineal behavior for  $\eta=1/2$  was obtained, indicating that the material behaves as a direct bandgap semiconductor. The band to band energy gap ( $E_g$ ) was calculated excluding the Urbach zone of the curve.

## References

---

1. P.-E. Werner, L. Eriksson and M. Westdahl, *J. Appl. Crystallogr.* 1985, **18**, 367.
2. A. Boultif and D. Louer, *J. Appl. Crystallogr.* 2004, **37**, 724.
3. A. Le Bail, H. Duroy and J.L. Fourquet, *Mat. Res. Bull.* 1988, **23**, 447.
4. J. Rodríguez-Carvajal, *Phys. B: Condens. Matter* 1993, **192**, 55.
5. A. Altomare, M. Camalli, C. Cuocci, C. Giacovazzo, A. Moliterni and R. Rizzi, *J. Appl. Crystallogr.* 2009, **43**, 798.
6. P. S. Bagus, E. S. Ilton and C. J. Nelin, *Surf. Sci. Rep.* 2013, **68**, 273.
7. P. M. Seah, "Quantification in AES and XPS", In Editor Briggs, D. and Grant, J. T., "Surface Analysis by Auger and X-ray Photoelectron Spectroscopy". Chichester, 2012, 345-375.